

A major purpose of the Technical Information Center is to provide the broadest dissemination possible of information contained in DOE's Research and Development Reports to business, industry, the academic community, and federal, state and local governments.

Although a small portion of this report is not reproducible, it is being made available to expedite the availability of information on the research discussed herein.

1

LA-UR
CONF-890406--20

Received by OSTI

JUN 07 1989

Los Alamos National Laboratory is operated by the University of California for the United States Department of Energy under contract W-7405-ENG-36

LA-UR--89-1747

DE89 013435

TITLE THEORY OF NEUTRON EMISSION IN FISSION

AUTHOR(S) David G. Madland, T-2

SUBMITTED TO The American Nuclear Society for publication in Proceedings of the ANS Conference, "Fifty Years with Nuclear Fission," April 26-28, 1989, National Bureau of Standards, Gaithersburg, MD.

DISCLAIMER

This report was prepared as an account of work sponsored by an agency of the United States Government. Neither the United States Government nor any agency thereof, nor any of their employees, makes any warranty, express or implied, or assumes any legal liability or responsibility for the accuracy, completeness, or usefulness of any information, apparatus, product, or process disclosed, or represents that its use would not infringe privately owned rights. Reference herein to any specific commercial product, process, or service by trade name, trademark, manufacturer, or otherwise does not necessarily constitute or imply its endorsement, recommendation, or favoring by the United States Government or any agency thereof. The views and opinions of authors expressed herein do not necessarily state or reflect those of the United States Government or any agency thereof.

By acceptance of this article the publisher recognizes that the U.S. Government retains a nonexclusive, royalty-free license to publish or reproduce the principal results of this contribution or to allow others to do so for U.S. Government purposes.

The U.S. National Laboratory requests that the publisher identify this article as work performed under the auspices of the U.S. Department of Energy.

 Los Alamos Los Alamos National Laboratory
Los Alamos, New Mexico 87545

MASTER

THEORY OF NEUTRON EMISSION IN FISSION

DAVID G. MADLAND
Theoretical Division
Los Alamos National Laboratory
Los Alamos, New Mexico 87545
(505) 667-6007

ABSTRACT

Following a summary of the observables in neutron emission in fission, a brief history is given of theoretical representations of the prompt fission neutron spectrum $N(E)$ and average prompt neutron multiplicity $\bar{\nu}_p$. This is followed by descriptions, together with examples, of modern approaches to the calculation of these quantities including recent advancements. Emphasis will be placed upon the predictability and accuracy of the modern approaches. In particular, the dependence of $N(E)$ and $\bar{\nu}_p$ on the fissioning nucleus and its excitation energy will be discussed, as will the effects of and competition between first-, second- and third-chance fission in circumstances of high excitation energy. Finally, properties of neutron-rich (fission-fragment) nuclei are discussed that must be better known to calculate $N(E)$ and $\bar{\nu}_p$ with higher accuracy than is currently possible.

I. INTRODUCTION

Neutron emission in fission can be described in terms of several experimental observables. These include the following:

- A. the time dependence of neutron emission in fission,
- B. the energy spectrum of prompt fission neutrons $N(E)$, where E is the laboratory energy of the emitted neutron and "prompt" refers to neutron emission prior to the onset of any fission-fragment β -decay process,
- C. the average number (or multiplicity) of prompt neutrons emitted per fission $\bar{\nu}_p$,
- D. the prompt fission neutron multiplicity distribution $P(\nu)$,
- E. the correlations and/or anti-correlations in neutron emission from complementary fragments,
- F. the energy spectrum of pre-fission neutrons $\phi(E)$ emitted prior to fission in multiple-chance fission,
- G. scission neutrons, and
- H. neutron emission from *accelerating* fragments in contrast to neutron emission from *fully accelerated* fragments.

While this list is not exhaustive, it does include most of the types of measurements that have been performed. In the present paper, items (B) and (C), the prompt fission neutron spectrum $N(E)$ and average prompt neutron multiplicity $\bar{\nu}_p$, will be emphasized for both spontaneous and neutron-induced fission.

In Sec. II a brief history will be presented, while in Sec. III three modern approaches will be described and examples given. Some recent work will be discussed in Sec. IV and a few conclusions will be presented in Sec. V.

II. EARLY REPRESENTATIONS

The prompt fission neutron spectrum $N(E)$ has been considered theoretically since the early days of fission by Feather,¹ Watt,² Leachman,³ Terrell,⁴ and others. Most calculations of $N(E)$, however, are to this day still based upon either a Maxwellian or Watt spectrum with parameters that are adjusted to optimally reproduce the experimental spectrum for a given fissioning system. At the same time, the variation of the average prompt neutron multiplicity $\bar{\nu}_p$ with the energy E_n of the neutron inducing fission has been modeled⁵ by a simple polynomial (usually linear) in E_n for each fissioning system considered: $\bar{\nu}_p = \nu_0 + \alpha E_n$, and again, the parameters appearing are adjusted to optimally reproduce the experimental multiplicity.

The Maxwellian spectrum is given by

$$N(E) = (2/\pi^{1/2}T_M^{3/2})E^{1/2}\exp(-E/T_M), \quad (1)$$

where the single (temperature) parameter appearing, T_M , is related to the average energy of the spectrum $\langle E \rangle$ by

$$\langle E \rangle = (3/2)T_M. \quad (2)$$

The Maxwellian spectrum neglects the *distribution* of fission-fragment excitation energy, the *energy dependence* of the inverse process of compound nucleus formation, and the *center-of-mass motion* of the fragments from which the neutrons are emitted. Because T_M must account for the fragment motion, it is *greater* than the fragment temperatures that physically occur. In practice, however, T_M is *reduced* in order to optimally reproduce the tail of the experimental spectrum. To preserve the normalization, this simultaneously increases $N(E)$ at lower energies. This increase at lower energies is in reasonable agreement with high quality measurements of the spectrum, *but for*

the wrong physical reason. For these reasons, there is no predictive power in a Maxwellian approach.

Feather,¹ in 1942, was the first to account for the motion of the fission fragments emitting the neutrons. He assumed the center-of-mass spectrum to be approximated by a Weisskopf evaporation spectrum⁶ and performed the transformation to the laboratory system. The resulting laboratory spectrum was expressed in terms of tabulated probability functions, and for this reason was not widely used.

Ten years later, in 1952, Watt² assumed the center-of-mass spectrum to be approximated by a Maxwellian spectrum. He then applied Feather's transformation to obtain the laboratory spectrum for an average fission fragment moving with an average kinetic energy per nucleon E_f . This yields the two-parameter Watt spectrum

$$N(E) = \frac{\exp(-E_f/T_w)}{(\pi E_f T_w)^{1/2}} \exp(-E/T_w) \sinh[2(E_f E)^{1/2}/T_w]. \quad (3)$$

where E_f and the Watt temperature T_w are related to the average energy of the spectrum $\langle E \rangle$ by

$$\langle E \rangle = E_f + (3/2) T_w. \quad (4)$$

Like the Maxwellian spectrum, the Watt spectrum neglects the distribution of fission-fragment excitation energy and the energy dependence of the inverse process of compound nucleus formation, but does account for the center-of-mass motion of an average fragment. However, the concept of an average fragment is a poor one for spontaneous and neutron-induced fission below about 15 MeV, because the fission-fragment mass distribution is dramatically double humped in most cases. Physically, then, there is an average kinetic energy per nucleon for the light mass peak, E_f^L , and for the heavy mass peak, E_f^H . Moreover, their magnitudes are well known from measurements of the total average fission-fragment kinetic energy $\langle E_f^{tot} \rangle$ together with the use of momentum conservation. Therefore in such cases, the Watt spectrum physically represents the contributions coming from a deep minimum in the fission-fragment mass yield distribution. In practice, however, the values of the two parameters, E_f and T_w , are adjusted to optimally reproduce the tail of the experimental spectrum. Thus, the Watt spectrum is more physical than a Maxwellian spectrum, but has little predictive power in most applications. If one insists on using a Watt spectrum representation, the average of the separate Watt spectra for the light and heavy mass peaks should be taken to represent the total laboratory spectrum $N(E)$.

To conclude this section, it is clear that none of the approaches summarized here can be used to predict $N(E)$ for a different fissioning nucleus or for a different excitation energy from what has been measured experimentally.

III. MODERN APPROACHES

In recent years three new theoretical approaches have evolved for the calculation of the prompt fission neutron spectrum $N(E)$. These are the following:

- A. The Los Alamos approach,⁷ begun in 1979, which is based upon standard nuclear evaporation theory⁶ and simultaneously treats the average prompt neutron multiplicity $\bar{\nu}_p$. This approach emphasizes predictive capabilities while requiring a minimal impact.
- B. The Dresden approach,⁸ began in 1982, which is also based upon standard nuclear evaporation theory,⁶ but accounts explicitly for neutron cascade emission. This approach emphasizes a complete description, requiring a substantial input.
- C. The Hauser-Feshbach statistical model approach, which is based upon Hauser-Feshbach theory⁹ and accounts explicitly for the competition between neutron and gamma-ray emission in a given fission fragment. This approach accounts for the influence of angular momentum.

Summary of Los Alamos Model

The original Los Alamos model⁷ addresses both neutron-induced and spontaneous fission and accounts for the physical effects of (1) the distribution of fission-fragment excitation energy, (2) the energy dependence of the inverse process of compound nucleus formation, (3) the center-of-mass motion of the fission fragments, and (4) multiple-chance fission at high incident neutron energy. In particular, to simulate the initial distribution of fission-fragment excitation energy and subsequent cooling as neutrons are emitted, a triangular approximation to the corresponding fission-fragment residual nuclear temperature distribution is used. This approximation, based upon the observations of Terrell,⁴ is given by

$$P(T) = \begin{cases} 2T/T_m^2 & T \leq T_m \\ 0 & T > T_m \end{cases} \quad (5)$$

where the maximum temperature T_m is related to the initial total average fission-fragment excitation energy $\langle E^* \rangle$ by

$$T_m = (\langle E^* \rangle / a)^{1/2}, \quad (6)$$

and where a is the nuclear level density parameter. In Eq. (6), the initial total average fission-fragment excitation energy is given by

$$\langle E^* \rangle = \langle E_f \rangle + E_n + B_n - \langle E_f^{tot} \rangle, \quad (7)$$

where $\langle E_f \rangle$ is the average energy release in fission, B_n and E_n are the separation and kinetic energies of the neutron inducing fission (set to zero for spontaneous fission), and $\langle E_f^{tot} \rangle$ is the total average fission-fragment kinetic energy. These quantities are either known or can be calculated.

The energy dependence of the inverse process is treated in the center-of-mass frame by calculating the compound nucleus formation cross section $\sigma_c(e)$ for the inverse process using an optical-model potential with explicit isospin dependence so as to describe (neutron rich) fission fragments more correctly. It is the shape of $\sigma_c(e)$ with e that affects $N(E)$.

The values of the average kinetic energy per nucleon of the average light fragment A_L and average heavy fragment A_H are obtained using momentum conservation and are given by

$$E_T^L = (A_H/A_L) (\langle E_T^{tot} \rangle / A) , \quad (8)$$

$$E_T^H = (A_L/A_H) (\langle E_T^{tot} \rangle / A) ,$$

where A is the mass number of the fissioning nucleus.

With the inclusion of these physical effects, the prompt fission neutron spectrum in the laboratory system is given by

$$N(E) = \frac{1}{2} [N(E, E_T^L, \sigma_c^L) + N(E, E_T^H, \sigma_c^H)] , \quad (9)$$

where

$$N(E, E_T, \sigma_c) = \frac{1}{2\sqrt{E_T} T_m^2} \int_{(\sqrt{E} - \sqrt{E_T})^2}^{(\sqrt{E} + \sqrt{E_T})^2} \sigma_c(e) \sqrt{e} de \int_0^{T_m} k(T) T \exp(-e/T) dT . \quad (10)$$

All quantities in this equation have been defined except $k(T)$, which is a temperature-dependent normalization. If $\sigma_c(e)$ is constant, Eq. (10) reduces to the closed form approximation

$$N(E, E_T) = \frac{1}{3(E_T T_m)^{1/2}} \left[u_2^{3/2} E_1(u_2) - u_1^{3/2} E_1(u_1) + \gamma\left(\frac{3}{2}, u_2\right) \cdot \gamma\left(\frac{3}{2}, u_1\right) \right] , \quad (11)$$

where

$$u_1 = (\sqrt{E} - \sqrt{E_T})^2 / T_m ,$$

$$u_2 = (\sqrt{E} + \sqrt{E_T})^2 / T_m ,$$

$E_1(x)$ is the exponential integral function, and

$\gamma(a, x)$ is the incomplete gamma function.

Similarly, the average prompt fission neutron multiplicity $\bar{\nu}_p$ is obtained from considerations of energy conservation and is given by

$$\bar{\nu}_p = \frac{\langle E^* \rangle - \langle E_T^{tot} \rangle}{\langle S_n \rangle + \langle e \rangle} , \quad (12)$$

where $\langle E_T^{tot} \rangle$ is the total average prompt gamma-ray energy, $\langle S_n \rangle$ is the average fission-fragment neutron separation energy, and $\langle e \rangle$ is the average center-of-mass energy of the emitted neutrons.

There are two specific connections between $N(E)$ and $\bar{\nu}_p$ that are worth noting. The first is that the maximum temperature T_m appearing as one of three parameters in $N(E)$ also appears in $\bar{\nu}_p$ as T_m^2 , through Eq. (6). The second is that the average center-of-mass neutron energy $\langle e \rangle$ appearing in $\bar{\nu}_p$ is also the first moment of the center-of-mass neutron spectrum $\Phi(e)$ corresponding to the laboratory spectrum $N(E)$. These two connections are very important because they mean that, if one has experimental information on either $N(E)$ or $\bar{\nu}_p$ for a given fissioning system, then that information can be used as a constraint in the calculation of the other, unmeasured, observable.

Examples of calculations performed using the original Los Alamos model are shown in Figs. 1-7. The numerical details and evaluation of the constants appearing in these calculations are found in Ref. 7 so they are not repeated here. First, comparisons of the Los Alamos spectrum for a constant cross section to Maxwellian and Watt spectra for the same fissioning system are shown in Figs. 1 and 2. The first moments (mean laboratory neutron energies) of the three spectra have been constrained to be identical by determining the Maxwellian and Watt temperatures, T_M and T_W , in terms of the physically based value of T_m . Using this basis for comparison, the Los Alamos spectrum lies between the Maxwellian and Watt spectra. The fact that T_M includes the effects of fragment motion is evident in Fig. 2, where the tail of the Maxwellian spectrum is clearly too hard due to the overly large value of T_M . The converse is true for the tail of the Watt spectrum, which is too soft because T_W is less than T_m .

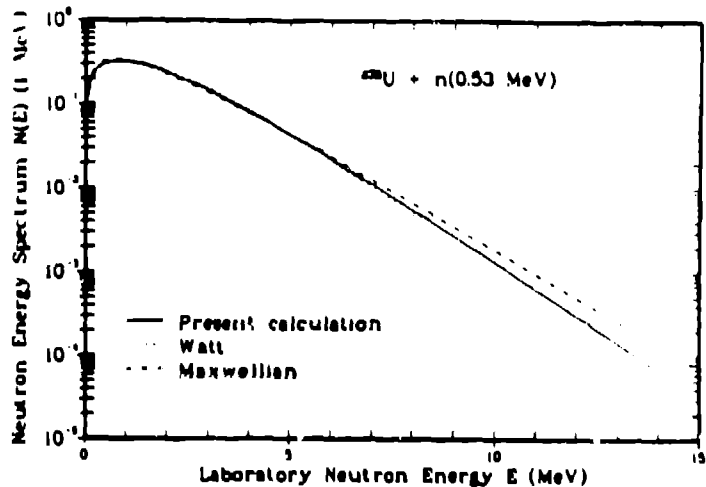


Fig. 1. Prompt fission neutron spectrum for the fission of ^{235}U induced by 0.53-MeV neutrons. The solid curve gives the Los Alamos spectrum calculated from Eqs. (9) and (11), for $\sigma_c(e) = \text{constant}$; the dashed curve gives the Watt spectrum calculated from Eq. (3); and the dot-dashed curve gives the Maxwellian spectrum calculated from Eq. (1). The mean laboratory neutron energies of the three spectra are identical.

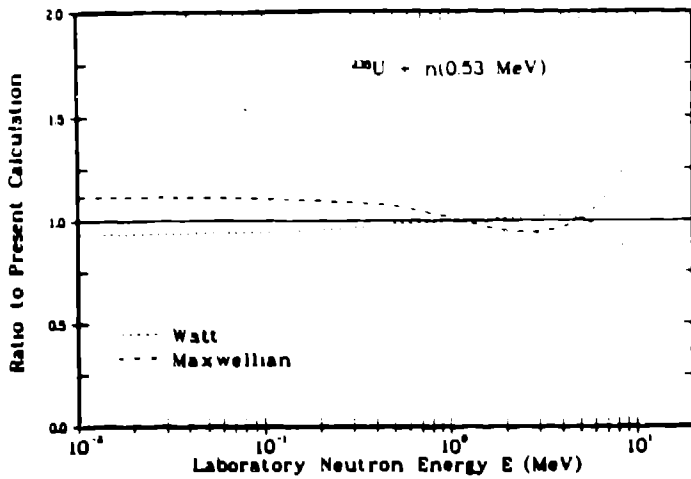


Fig. 2. Ratio of the Watt spectrum and the Maxwellian spectrum to the Los Alamos spectrum, corresponding to the curves shown in Fig. 1.

The dependence of $N(E)$ on the fissioning nucleus and its excitation energy is shown for the constant cross section Los Alamos model in Figs. 3 and 4. Figure 3 shows how the spectrum increases at high energy and decreases at low energy as the mass and charge of the fissioning nucleus increases, for thermal-neutron-induced fission. Thus, $\langle E_T \rangle$ is increasing faster with the mass of the fissioning nucleus than $\langle E_{f_0} \rangle$ is increasing with the charge of the fissioning nucleus [see Eqs. (6) and (7)]. Similarly, Fig. 4 shows how the spectrum increases at high energy and decreases at low energy as the kinetic energy of the incident neutron increases, for the first-chance fission of ^{235}U .

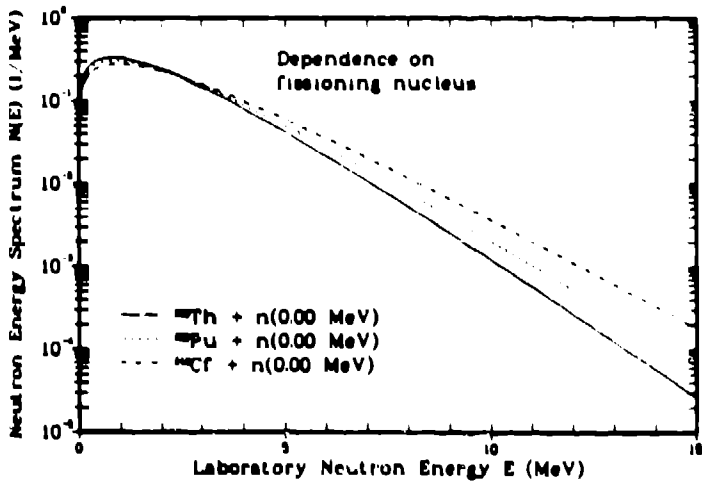


Fig. 3. Dependence of the prompt fission neutron spectrum on the fissioning nucleus, for thermal-neutron-induced fission, calculated using the Los Alamos model, Eqs. (9) and (11), for $\sigma_c(E) = \text{constant}$.

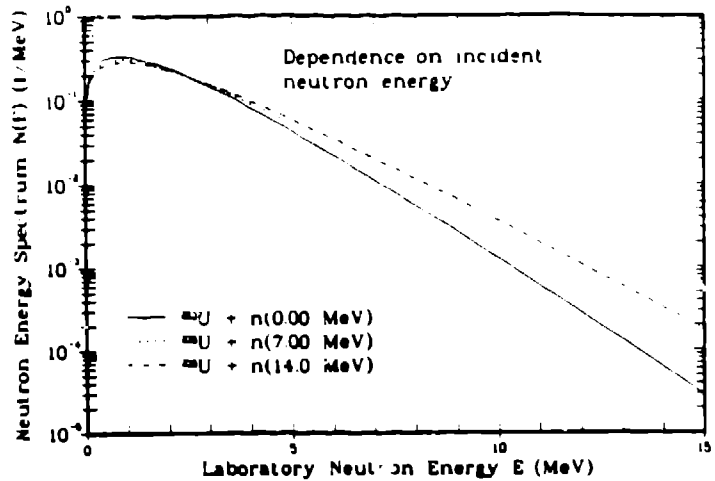


Fig. 4. Dependence of the prompt fission neutron spectrum on the kinetic energy of the incident neutron for the fission of ^{235}U , calculated using the Los Alamos model, Eqs. (9) and (11), for $\sigma_c(E) = \text{constant}$.

Figures 5 and 6 compare both the exact and approximate versions of the Los Alamos spectrum with experimental data. Clearly, there is a preference for the exact energy-dependent cross-section calculation, although both agree well with the experiment. Thus, given the quality of the experimental data, the Los Alamos exact spectrum given by Eqs. (9) and (10) is to be used when high accuracy is required. In such cases, the energy dependence of the inverse process of compound nucleus formation cannot be ignored.

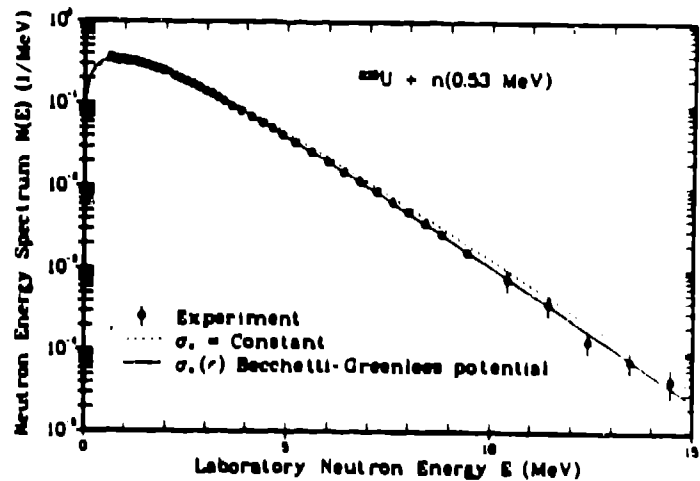


Fig. 5. Prompt fission neutron spectrum for the fission of ^{235}U induced by 0.53-MeV neutrons. The dashed curve gives the Los Alamos spectrum calculated from Eqs. (9) and (11), for $\sigma_c(E) = \text{constant}$, whereas the solid curve gives the Los Alamos spectrum calculated from Eqs. (9) and (10), for $\sigma_c(E)$ obtained using the optical-model potential of Becchetti and Greenless (Ref. 10). The experimental data are those of Johansson and Holmqvist (Ref. 11).

Summary of Dresden Model

The Dresden model⁸ accounts for the physical effects of (1) the distribution of fission-fragment excitation energy in each step of the cascade evaporation of neutrons, (2) the energy dependence of the inverse process of compound nucleus formation, (3) the center-of-mass motion of the fission fragments, (4) the anisotropy of the center-of-mass neutron spectrum, (5) the complete fission-fragment mass and kinetic-energy distributions, and (6) semi-empirical fission-fragment nuclear level densities. The Dresden model is currently referred to as the Complex Cascade Evaporation Model.

With the inclusion of the above physical effects in sufficient detail, the prompt fission neutron spectrum in the laboratory system is given by

$$N(E) = \sum_A \int P(A, TKE) N(E, A, TKE) dTKL, \quad (13)$$

where $P(A, TKE)$ is the normalized fission-fragment mass distribution for a fixed value of the total fission-fragment kinetic energy, TKE , and $N(E, A, TKE)$ is the laboratory spectrum for fixed fragment mass A and fixed TKE . The sum and integral are over all contributing fragment mass numbers and total kinetic energies, respectively. The fragment spectrum $N(E, A, TKE)$ is given by

$$N(E, A, TKE) = \int \frac{\phi(\epsilon, A, TKE)}{4\sqrt{\epsilon E_f}} \left\{ \frac{1 + b[(E - E_f - \epsilon)^2 / 4\epsilon E_f]}{1 + (b/3)} \right\} d\epsilon, \quad (14)$$

where E_f is the kinetic energy per nucleon of the fragment, b is the anisotropy coefficient, ϵ is the center-of-mass neutron energy, and $\phi(\epsilon, A, TKE)$ is the center-of-mass spectrum for fixed fragment mass and fixed TKE , given by

$$\phi(\epsilon, A, TKE) = \sum_{B_i} \int_{B_i}^{\infty} \phi_i(\epsilon, E^*, A-i) P_i(E^*, A, TKE) dE^*. \quad (15)$$

In this equation, the sum is over the steps i of the cascade while the integral is over the fragment excitation energy E^* , and B_i is the neutron binding energy in a fragment that has emitted i neutrons. Also, $P_i(E^*, A, TKE)$ is the excitation energy distribution before step i and is expressed in terms of P_{i-1} and, ultimately, P_0 , which is assumed Gaussian. Finally, $\phi(\epsilon, E^*, A)$ is the Weiskopf⁶ center-of-mass neutron energy spectrum for fixed E^* and A , given by

$$\phi(\epsilon, E^*, A) = C \sigma_0(\epsilon, A-1) \epsilon \rho(E^* - B_n - \epsilon, A-1), \quad (16)$$

where ρ is the level density of the residual nucleus for zero angular momentum states and C is the normalization constant.

Examples of calculations performed using the Dresden (Complex Cascade Emission) model are shown in Figs. 8 and 9 for the spontaneous fission of ²⁵²Cf. The numerical details and evaluation of the constants appearing in these calculations are found in Refs. 12 and 13 so they are not repeated here. The reality of anisotropy effects in the prompt fission neutron spectrum is demonstrated in Fig. 8 where recent experimental

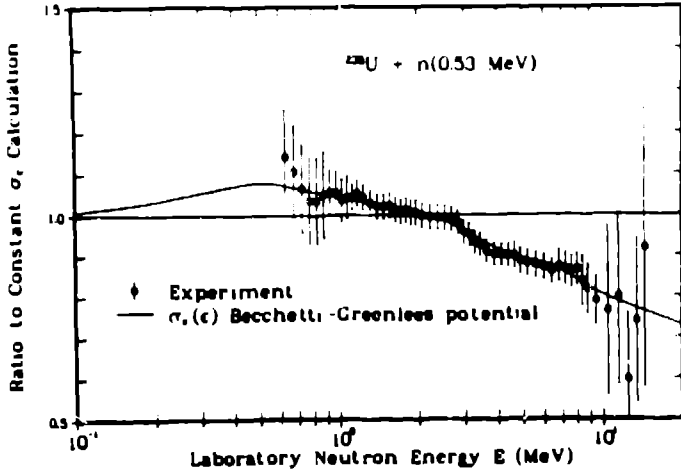


Fig. 6. Ratio of the Los Alamos spectrum calculated using energy-dependent cross sections and the experimental spectrum to the Los Alamos spectrum calculated using a constant cross section, corresponding to the curves shown in Fig. 5.

Turning to the calculation of the average prompt neutron multiplicity $\bar{\nu}_p$ using the Los Alamos model, Fig. 7 shows a comparison of calculated and experimental values of $\bar{\nu}_p$ for the neutron-induced fission of ²³⁵U. The agreement is better than 1% at energies below 1 MeV and at 6 MeV. In the region from ~ 1.5 to 5.5 MeV, however, the experimental values are somewhat less than the calculated values, ~ 3% differences at 4.5 MeV. Nevertheless, the agreement between experiment and calculation is quite good, given the approximations implied by the use of averaged quantities in Eq. (12).

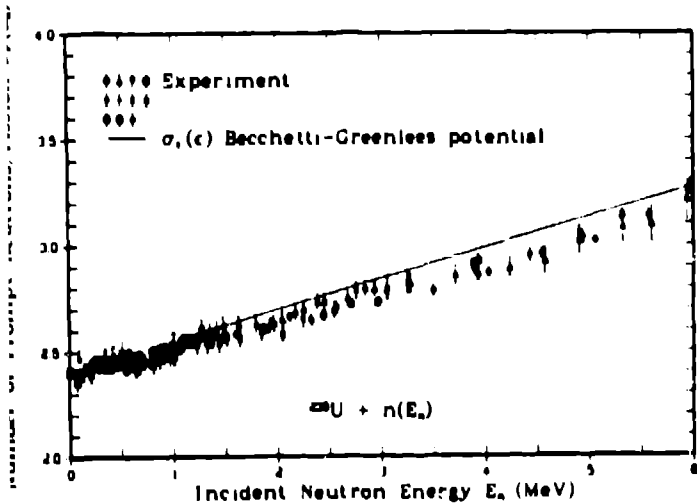


Fig. 7. Average prompt neutron multiplicity as a function of the incident neutron energy for the neutron-induced fission of ²³⁵U. The solid curve gives the Los Alamos multiplicity calculated with Eq. (12) using the optical-model potential of Becchetti and Greenlees (Ref. 10) to calculate the average center-of-mass energy $\langle \epsilon \rangle$. The experimental data are listed in Ref. 7.

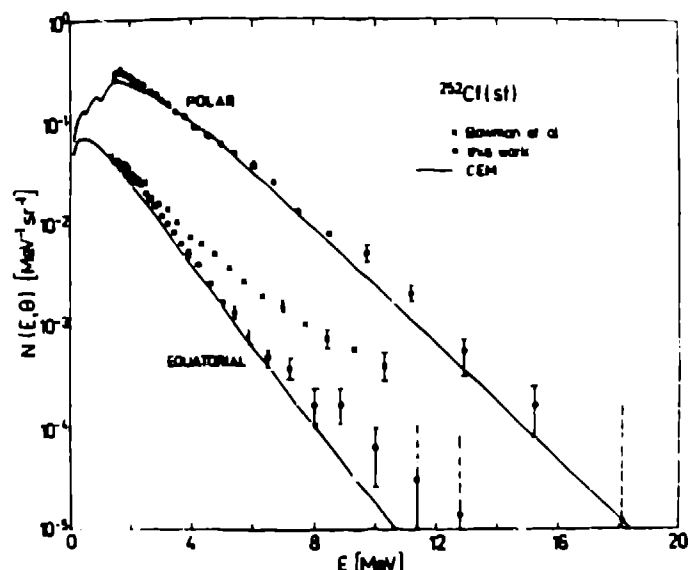


Fig. 8. Prompt fission neutron spectra for the spontaneous fission of ^{252}Cf in the parallel (polar) and perpendicular (equatorial) directions with respect to the fission axis. The experimental data are from Ref. 12 (closed circles) and Ref. 14 (crosses). The solid curves are calculated using the Dresden model, Eqs. (13)-(16), but without integration over angle.

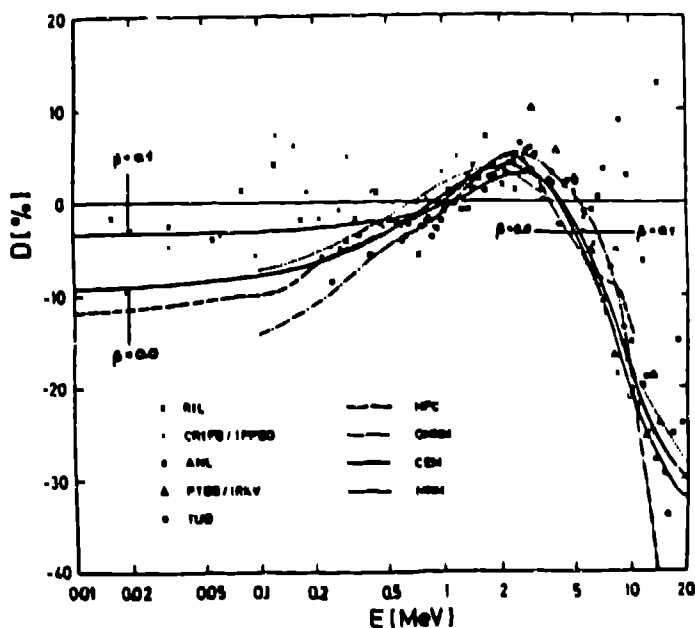


Fig. 9. Prompt fission neutron spectra for the spontaneous fission of ^{252}Cf shown as the deviation, in per cent, from a Maxwellian spectrum with $T_M = 1.42$ MeV. The solid curves are calculated using the Dresden model (CEM), Eqs. (13)-(16), for two values of the anisotropy coefficient b (β in the figure). The experimental data points shown are from the indicated laboratories, but the experimental uncertainties have been deleted for clarity.

data for polar and equatorial emission, and calculations using the Dresden model with an anisotropy coefficient $b = 0.1$, agree well with each other. The experimental and calculated spectra for the same fissioning system, but integrated over all angles of neutron emission, are shown in Fig. 9 as deviations from a Maxwellian spectrum. Again, the Dresden model (CEM), solid curve for $b = 0.1$ ($\beta = 0.1$), yields quite good agreement with experiment especially at the low energy end of the spectrum. Clearly, the anisotropy of the center-of-mass spectrum must be taken into account to obtain the most realistic representation of the experimental spectrum.

Summary of Hauser-Feshbach Approach

This approach consists of Hauser-Feshbach statistical model calculations of the de-excitation of representative nuclei of the fission-fragment mass and charge distributions. This model applied to fission fragments accounts for the physical effects included in the Los Alamos and Dresden models and, in addition, accounts for (1) neutron and gamma-ray competition in the de-excitation of a given fission fragment, (2) neutron transmission coefficients T_{nj} from an optical model potential for each fragment considered, (3) gamma-ray transmission coefficients T_γ for each fragment considered, and (4) the angular momentum distribution $P(J)$ for each fragment considered.

Due to space limitations, a detailed description of the Hauser-Feshbach formalism for de-excitation of fission fragments is not presented here. Instead the reader is referred to the work of Browne and Dietrich¹⁵ in 1974, where Hauser-Feshbach calculations are performed for 40 nuclei representing the fragment yield distribution from the $^{252}\text{Cf}(sf)$ reaction, and the work of Gerasimenko and Rubchenya¹⁶ in 1980, where Hauser-Feshbach calculations are performed for 18 nuclei representing the same reaction. In the latter calculation, quite good agreement with experiment is achieved when a center-of-mass anisotropy coefficient of $b = 0.15$ is used.

Ultimately, because of the treatment of neutron and gamma-ray competition, and the inclusion of angular momentum, the Hauser-Feshbach approach will probably provide the most accurate calculation of the prompt fission neutron spectrum. However, a proper description of the initial fission-fragment conditions (for the ~ 300 fragments occurring) is a prerequisite.

IV. RECENT WORK

One example of recent work is discussed briefly in this section to illustrate the effects of multiple-chance fission. Figures 10 and 11 show the prompt fission neutron spectrum matrix $N(E, E_n)$ for the neutron-induced fission of ^{235}U up through 3rd-chance fission. The exact energy-dependent Los Alamos spectrum, Eqs. (9) and (10), is utilized together with evaporation spectra to describe the emission of neutrons prior to fission. Various features of this calculation have previously been described in Refs. 7 and 17. The figures clearly illustrate the dependence of the matrix upon E_n . In particular, the partition of the total available excitation energy into neutron emission prior to fission and neutron emission from fission fragments leads to a staircase effect in the peak regions of the matrix and an oscillatory effect in the tail regions of the matrix.

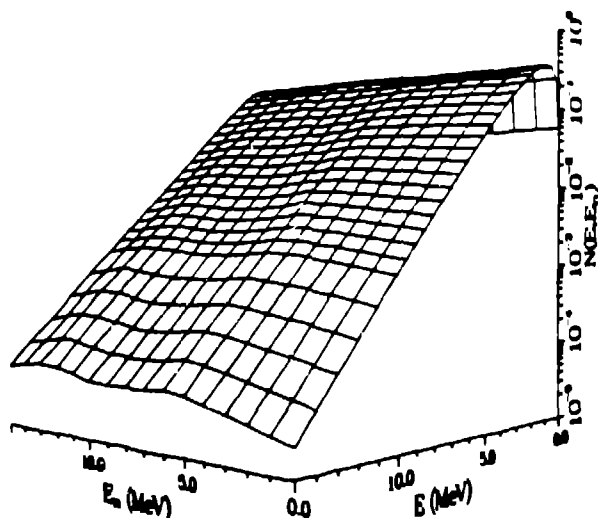


Fig. 10. Prompt fission neutron spectrum matrix $N(E, E_n)$ for the neutron-induced fission of ^{235}U as a function of incident neutron energy E_n and emitted neutron energy E .

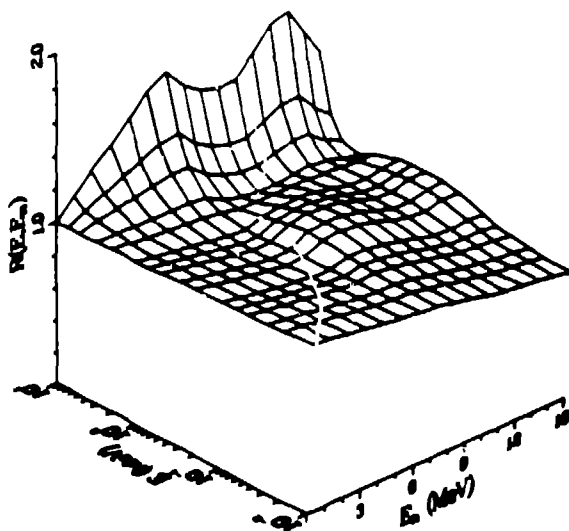


Fig. 11. Prompt fission neutron spectrum ratio matrix $R(E, E_n) = N(E, E_n)/N(E, 0)$, corresponding to the matrix shown in Fig. 10.

V. CONCLUSIONS

Three conclusions can be drawn from the theoretical studies to date on the topics discussed herein. These are:

- A. Prompt fission neutron spectra and average prompt neutron multiplicities can now be calculated with reasonably good confidence for unmeasured as well as measured systems, and for spontaneous as well as neutron-induced fission.
- B. Ultimately, the Hauser-Feshbach approach will probably yield the most accurate results.
- C. Current limitations in calculations are due to poor descriptions of neutron-rich nuclei. In particular, more accurate nuclear level densities, optical-model

potentials with isospin dependence, and ground-state masses are required. Also, explicit fission-fragment properties that are required with higher accuracy include initial excitation energy distributions and initial angular momentum distributions.

REFERENCES

1. N. FEATHER, "Emission of Neutrons from Moving Fission Fragments," BM-148, British Mission (1942).
2. B. E. WATT, Phys. Rev., **87**, 1037 (1952).
3. R. B. LEACHMAN, Phys. Rev., **101**, 1005 (1956).
4. J. TERRELL, Phys. Rev., **113**, 527 (1959).
5. F. MANERO and V. A. KONSHIN, Atomic Energy Rev., **10**, 637 (1972).
6. V. F. WEISSKOPF, Phys. Rev., **52**, 295 (1937).
7. D. G. MADLAND and J. R. NIX, Nucl. Sci. Eng., **81**, 213 (1982) and earlier references contained therein.
8. H. MÄRTEN and D. SEELIGER, J. Phys. G., **10**, 349 (1984) and earlier references contained therein.
9. W. HAUSER and H. FESHBACH, Phys. Rev., **87**, 366 (1952).
10. F. D. BECCHETTI, JR. and G. W. GREENLEES, Phys. Rev., **182**, 1190 (1969).
11. P. I. JOHANSSON and B. HOLMQVIST, Nucl. Sci. Eng., **52**, 695 (1977).
12. D. SEELIGER, H. MÄRTEN, W. NEUBERT, and D. RICHTER, Sov. J. Nucl. Phys., **47**, 403 (1988).
13. H. MÄRTEN and D. SEELIGER, "Measurement and Theoretical Calculation of the ^{252}Cf Spontaneous-Fission Neutron Spectrum" in Proc. Advisory Group Mtg. Nuclear Standard Reference Data, Geel, Belgium, 1984 (IAEA-TECDOC-335, Vienna, 1985), p. 255.
14. H. R. BOWMAN, S. G. THOMPSON, J. C. D. MILTON, and W. J. SWIATECKI, Phys. Rev., **126**, 2120 (1962).
15. J. C. BROWNE and F. S. DIETRICH, Phys. Rev. C, **10**, 2545 (1974).
16. B. F. GERASIMENKO and V. A. RUBCHENYA, "Theoretical Calculations of Prompt Neutron Spectrum for Cf-252 Spontaneous Fission," in Proc. Advisory Group Mtg. Properties of Neutron Sources, Leningrad, USSR, 1986 (IAEA-TECDOC-410, Vienna, 1987), p. 208.
17. D. G. MADLAND, R. J. LABAUVE, and J. R. NIX, "Recent Improvements in the Calculation of Prompt Fission Neutron Spectra: Preliminary Results," IAEA Consultants' Mtg. on the Physics of Neutron Emission in Fission, Mito, Japan, May 24-27, 1988 (in press).